1   Clarifying intercellular signalling in yeast: *Saccharomyces cerevisiae* does not

2   undergo a quorum sensing-dependent switch to filamentous growth

3   Michela Winters[a], Violetta Aru[b], Kate Howell[a,#], and Nils Arneborg[b]

4   [a] School of Agriculture and Food, Faculty of Veterinary and Agricultural Science,

5   University of Melbourne, Parkville 3010, Australia

6   [b] Department of Food Science, University of Copenhagen, Frederiksberg 1958,

7   Denmark

8

9   Running Head (max 54 characters & spaces): Unipolar budding of *Saccharomyces*

10   *cerevisiae*

11

12   #Address correspondence to Kate Howell, khowell@unimelb.edu.au

13

14   Abstract word count: 249 (max 250)

15   Importance: 150 (max 150 words)

16   Text Word Count: 5028 (5000 approx limit)

17

ABSTRACT (250 WORDS)

Saccharomyces cerevisiae can alter its morphology to a filamentous form associated with unipolar budding in response to environmental stressors. Induction of filamentous growth is suggested under nitrogen deficiency in response to alcoholic signalling molecules through a quorum sensing mechanism. To investigate this claim, we analysed the budding pattern of *S. cerevisiae* cells over time under low nitrogen while concurrently measuring cell density and extracellular metabolite concentration. We found that the proportion of cells displaying unipolar budding increased between local cell densities of 4.8×10^6 and 5.3×10^7 cells/ml within 10 to 20 hours of growth. However, the observed increase in unipolar budding could not be reproduced when cells were prepared at the critical cell density and in conditioned media. Removing the nutrient restriction by growth in high nitrogen conditions also resulted in an increase in unipolar budding between local cell densities of 5.2×10^6 and 8.2×10^7 cells/ml within 10 to 20 hours of growth, but there were differences in metabolite concentration compared to the low nitrogen conditions. This suggests that neither cell density, metabolite concentration, nor nitrogen deficiency were necessary or sufficient to increase the proportion of unipolar budding cells. It is therefore unlikely that quorum sensing is the mechanism controlling the switch to filamentous growth in *S. cerevisiae*. Only a high concentration of the putative signalling molecule, 2-phenylethanol resulted in an increase in unipolar budding, but this concentration was not physiologically relevant. We suggest that the compound 2-phenylethanol acts through a toxicity mechanism, rather than quorum sensing, to induce filamentous growth.

IMPORTANCE (150 WORDS)

40

41   Investigating dimorphism in the model organism *Saccharomyces cerevisiae* has

42   been instrumental in understanding the signalling pathways that control hyphal growth

43   and virulence in human pathogenic fungi. Quorum sensing was proposed to signal

44   morphogenesis in *S. cerevisiae* populations. This mechanism requires the switch to

45   filamentous growth to occur at a critical quorum sensing molecule concentration

46   corresponding to a critical cell density. However, the evidence for this mechanism is

47   sparse and limited by the use non-physiologically relevant concentrations of signalling

48   metabolites. Our study designed a methodology to address this gap and may be applied

49   to further studies of dimorphism in other types of yeasts. A significant implication of our

50   findings is that morphogenesis does not occur in *S. cerevisiae* via a quorum sensing

51   mechanism, and this important definition needs to be corrected. Mechanistic studies to

52   understand dimorphism in yeasts, by considering metabolite concentrations, will further

53   shed light onto this important cellular behaviour.

KEYWORDS

54

55   *Saccharomyces cerevisiae,* filamentous growth, budding pattern, signalling

56   metabolites, cell density

INTRODUCTION

57

58   The yeast *Saccharomyces cerevisiae* has the ability to exist in different

59   multicellular forms depending on its environment. In liquid environments, the yeast cells

60   can be sessile or planktonic and may form flocs and flors, and in solid and semi-solid

61   substrates, colonies, biofilms, filaments and mats are observed. Filamentous growth of

3

62   *S. cerevisiae* commonly occurs under nutrient starvation and has been hypothesised as

63   a mechanism to allow the cells to grow into their immediate environment and forage for

64   available nutrients (1, 2). This morphogenesis is described as pseudohyphal or invasive

65   depending on whether the cells exist as diploids or haploids and can be observed both

66   at a colony and cellular level. When growing on agar plates, colony morphology and

67   invasion reveal filamentous growth, and these macro-observations are determined by

68   budding pattern and cell shape that indicate filamentous growth at the cellular level.

69   Budding is the method by which *S. cerevisiae* cells divide during their mitotic cell

70   cycle. The budding pattern is determined by the orientation of new buds with respect to

71   the mother-daughter junction and can be differentiated as axial, bipolar or unipolar (Fig.

72   1A). Whether the cell is a diploid or haploid will determine which budding pattern is

73   exhibited when cells grow planktonically (3, 4). Haploid cells bud in an axial manner

74   whereby the new bud consistently emerges adjacent to or overlapping the pole of the

75   previous mother-daughter junction. Diploid cells, however, bud according to a bipolar

76   pattern, where buds can emerge either adjacent to the mother-daughter junction or at

77   the opposite pole. Usually, the first bud site of a new daughter cell has a strong opposite

78   pole bias, while second and subsequent buds have no bias towards a pole (1, 3, 5, 6).

79   Both haploids and diploids transition to a unipolar budding pattern when cells switch to

80   filamentous growth. This pattern occurs when the daughter buds consistently from the

81   pole opposite the junction to its mother (1, 7-11). Cell division is thus polarized by the

82   serial reiteration of unipolar budding away from the mass of cells in the colony into

83   chains of interconnected cells (1).

84   *S. cerevisiae* cells undergoing filamentous growth have a higher proportion of

85   unipolar budding compared to non-filamentous cells. Previous research established that

86   when two bud sites are observed, non-filamentous cells show 70-71% unipolar budding,

87   while filamentous cells show 90-100% unipolar budding (1, 7). For cells with three bud

88   sites, this proportion of unipolar budding was observed to be 26% for non-filamentous

89   cells and 97% for filamentous cells (7). Furthermore, under filamentous growth inducing

90   conditions (nitrogen deficiency), unipolar budding was found to increase by an average

91   of 35% (12). Observation of a higher proportion of unipolar budding cells thus signifies

92   that cells are on track to grow as filaments.

93   Filamentous growth is induced in *S. cerevisiae* cells in response to different

94   environmental cues and stressors, including nutrient deficiency and signalling

95   molecules. Filamentous cells are considered more able to scavenge nutrients when

96   exposed to a variety of extracellular stressors (13). Nutrient starvation, including lack of

97   nitrogen (1, 11, 14-16), glucose (8, 17), carbon (16) and amino acids (18), can trigger

98   the morphological change to filamentous growth. An additional adaptation to nitrogen

99   starvation is the secretion of autoregulatory aromatic alcohols that stimulate filamentous

100   growth through a quorum sensing mechanism (14, 19-21).

101   Quorum sensing is a form of intercellular signalling where interactions between

102   organisms are mediated by intercellular signalling molecules (22). Quorum sensing

103   involves a cell-density dependent regulation of a behaviour that occurs after a critical

104   signal concentration of quorum sensing molecules is achieved (23). Quorum sensing

105   molecules are excreted and accumulate in the extracellular environment proportional to

106   cell density. At the critical cell density a corresponding threshold concentration of

107   quorum sensing molecules is reached and a synchronised response is triggered in the

108   community of cells (24-29). H. Chen and G. R. Fink (14) observed a quorum sensing-

109   controlled mechanism for the switch to filamentous growth in *S. cerevisiae,* connecting

110   nutrient sensing with aromatic alcohol secretion. Nitrogen and cell density were

111   demonstrated to regulate the production of three auto-induced aromatic alcohols via a

112   positive feedback loop. These included tyrosol (produced in the range 1-8 µM), 2-

113   phenylethanol (in the range of 1-8 µM) and tryptophol (in the range 1-2 µM). 2-

114   phenylethanol and tryptophol, but not tyrosol, were then found to stimulate filamentous

115   growth when added exogenously at ≥20 µM under nitrogen limiting conditions. Further

116   studies have linked exogenous addition of different alcohols to induction of

117   morphogenesis under both high (30) and low nitrogen (11) conditions. These include 1-

118   butanol (11), isoamylol (11, 30), 1-propanol (11, 30) and n-hexanol (30). However, all

119   these studies induced morphogenesis by using exogenous alcohol concentrations much

120   higher than those found to be produced when the cell is growing in defined or undefined

121   media (23).

122   Intercellular signalling interactions need to be defined by specific criteria to be

123   accurately identified and understood. Previous definitions of quorum sensing have

124   tended to be very broad so that any morphological behaviours in yeast may have been

125   inaccurately categorised as being a result of quorum sensing. In our previous work, M.

126   Winters et al. (23) set out a series of criteria for what constitutes an intercellular

127   signalling molecule and quorum sensing molecule to promote clarity in classifying

128   microbial interactions. When these defined criteria were applied to studies of quorum

129   sensing-controlled filamentous growth in *S. cerevisiae* we found that two criteria were

130   consistently not met in prior research (23). Firstly, there is a lack of evidence that the

131   switch in cellular behaviour occurs at a critical quorum sensing molecule concentration

132   corresponding to a critical cell density. Secondly, all studies analysed did not use

133   physiologically relevant concentrations of intercellular signalling molecules to trigger the

134   switch to filamentous growth.

135   In the current study, we aimed to address these two missing criteria on the role of

136   quorum sensing in the switch to filamentous growth in *S. cerevisiae*. We designed a

137   new methodology which uses budding pattern as a proxy for filamentous growth. This

138   involved observing an individual cell, growing over time, to determine the orientation of

139   buds from new daughter cells. By using an oCelloScope^{TM} to capture time-lapse images

140   of budding yeast growing in liquid media, we observed a switch to a filamentous

141   budding pattern. Since our method simultaneously quantified the budding pattern, cell

142   density and metabolite concentration under physiological conditions, we successfully

143   identified the critical cell density and metabolite concentration at which cells switched to

144   filamentous growth. An untargeted metabolome approach through proton (^{1}H) NMR

145   meant both previously reported and putative quorum sensing molecules could be

146   monitored. Next, we individually assessed the role of cell density, metabolites, and

147   nitrogen concentration in triggering this switch to filamentous growth. Additionally, we

148   investigated the role of exogenous addition of 2-phenylethanol, a putative quorum

149   sensing molecule, in morphogenesis and found it only induced a change in morphology

150   at high non-physiological concentrations. Together, our findings suggest that *S.*

151   *cerevisiae* does not undergo a quorum sensing-dependent switch to filamentous growth,

152   and that 2-phenylethanol acts through a toxicity mechanism rather than as a quorum

153   sensing molecule. Finally, the novel methodology developed here opens the way for

154   further studies of dimorphism in other strains and species of yeasts.

RESULTS

155

156   *S. cerevisiae* Σ1278b displays a switch in budding pattern under low nitrogen.

157   We designed a time series experiment such that *S. cerevisiae* strains could grow

158   in the same media continuously to obtain an accurate link between our three factors of

159   interest: budding pattern, cell density and metabolite concentration. The cropped

160   images obtained from the oCelloScope™ were analyzed manually and the bud site

161   sequence of new daughters were recorded followed by a classification of their

162   corresponding budding pattern (Fig. 1A). A representative example of this assignment

163   process can be seen in Figure 1B.

164   The growth of *S. cerevisiae* strains S288c and Σ1278b were observed under low

165   nitrogen conditions over 30 hours (Fig. 2). The cells grew logarithmically throughout the

166   duration of the experiment such that they were only followed in their exponential growth

167   phase (Fig. 2A). At 30 hours, S288c continues to grow exponentially, while the Σ1278b

168   strain growth rate begins to decline after 20 hours. This decline is likely related to the

169   nitrogen starvation that occurred toward the end of the experiment (Table S1).

170   A predominantly axial budding pattern was observed for the negative control

171   strain S288c for both the two and three bud sites, with no significant changes in budding

172   pattern observed over time (Fig. 2 B). Strain Σ1278b budded in a predominantly bipolar

173   or unipolar pattern. Additionally, the proportion of unipolar budding was observed to

174   increase over time, with a corresponding decrease in bipolar budding, for both two and

8

175   three bud sites (Fig 2 D and E). An increase in the proportion of unipolar budding from

176   72% to 91% (Fig 2D) was observed in cells with two bud sites. For cells with three bud

177   sites, it increased from 20% to 36% (Fig 2E). Due to the growth limitation caused by

178   nitrogen starvation between 20 and 30 hours (Table S1) the cells were only able to

179   achieve two bud sites and therefore budding pattern data for three bud sites was not

180   available during this period (Fig 2E). The significant (P< 0.05) increase in filamentous

181   unipolar budding occurred between the local cell densities of $4.8x10^6$ and $5.3x10^7$

182   cells/ml within 10 and 20 hours of growth. These values signify the critical cell density

183   for the switch to filamentous growth.

184   **Change in budding pattern and identified critical cell density are correlated to the**

185   **physiological concentration of metabolites present.**

186   To correlate the change in concentration of metabolites over time to the changes

187   in budding pattern and cell density observed, media from the time series experiments

188   were collected, measured by ^{1}H NMR spectroscopy, and compounds identified and

189   quantified with SigMa (31). In total, 29 compounds were identified in the media with

190   concentrations quantified for each time period (Table 1).

191   The metabolite concentrations that corresponded to the observed switch in

192   budding pattern were 1-propanol (1.4 – 3.7 µM), 2-hydroxyisovalerate (0.7 – 1.3 µM), 2-

193   oxoglutarate (4.4 – 9.3 µM), 2-phenylethanol (0.7 – 1.5 µM), acetaldehyde (2.3 – 19.2

194   µM), acetate (17 - 160 µM), acetoin (6.7 – 8.0 µM), fumarate (0.5 – 1.1 µM), isoamylol

195   (0.6 – 1.0 µM), isopropanol (0.4 – 2.1 µM), malate (2.9 – 6.8 µM), pyruvate (5.0 – 30.6

196   µM), succinate (2.5 – 12.0 µM), and tyrosol (0.3 – 0.8 µM). These values represent the

197   physiological metabolite concentration present at the critical cell density at which cells

198   switch to filamentous growth.

Critical cell density does not recapitulate the switch in budding pattern.

200   To establish whether the increase in unipolar budding was dependent on cell

201   density alone, we inoculated cells at the critical cell density, recorded at 10 hours, into

202   low nitrogen media (Fig. 3). This cell density was chosen as it was at the beginning of

203   the time period where we observed the significant increase in unipolar budding. At the

204   critical cell density, 71% of cells with two bud sites had a unipolar pattern (Fig. 3A). This

205   was analogous to 72% unipolar budding observed between 0 to 10 hours in the time

206   series experiment (Fig. 2D). This parallel was also seen for cells with three bud sites at

207   the critical cell density where we measured 23% unipolar budding (Fig. 3B) compared to

208   20% between 0 to 10 hours in the time series results (Fig. 2E). Since the critical cell

209   density did not replicate the increase in unipolar budding, these findings demonstrate

210   that cell density alone is not responsible for the behaviour.

Conditioned media and cells at the critical cell density do not recapitulate the

switch in budding pattern.

213   To test whether the combination of physiological metabolites and the critical cell

214   density was a trigger for the increase in unipolar budding, we determined the budding

215   pattern of cells growing in conditioned media from 20 hours of growth at the critical cell

216   density in low nitrogen media (Fig. 3). Growth of cells with two bud sites in conditioned

217   media had 71% unipolar budding (Fig. 3A) and cells with three bud sites had 18% (Fig.

218   3B). The proportion of unipolar budding observed between the critical cell density and

219   conditioned media conditions were not significantly different; both had 71% for two bud

10

220 sites (Fig. 3A), and 20% and 18% respectively for three bud sites (Fig. 3B). In both

221 cases the values paralleled the proportion of unipolar budding observed between 0 to

222 10 hours in the time series experiment; 72% for two bud sites (Fig. 2D) and 20% for

223 three bud sites (Fig. 2E). Thus, the combination of critical cell density and physiological

224 metabolite concentrations were also not accountable for the observed increase in

225 unipolar budding.

226 **High nitrogen replicated the switch budding pattern but with different produced**

227 **metabolite concentrations.**

228   To determine whether budding pattern behaviour over time was impacted by

229 nitrogen conditions, we carried out the time series experiment in high nitrogen media.

230   Similar to growth in low nitrogen, S288c and Σ1278b cells grew logarithmically

231 throughout the duration of the experiment such that they were only followed in their

232 exponential growth phase (Fig. 4A). However, there was a less pronounced decrease in

233 growth rate for the Σ1278b compared to the S288c under high nitrogen conditions

234 compared to low nitrogen conditions. This can be explained by the absence of nitrogen

235 starvation under high nitrogen (Table S1).

236   Budding pattern behaviour was not significantly different between the two

237 nitrogen conditions. Just as in low nitrogen, S288c showed a predominantly axial

238 budding pattern with no changes over time (Fig. 4B and C) and Σ1278b showed a

239 consistently bipolar or unipolar budding pattern (Fig. 4D and E). Again, we saw a

240 significant increase to a unipolar budding pattern accompanied by a significant decrease

241 in bipolar budding between 10 and 20 hours for cells with both two and three bud sites

242 (Fig. 4D and E). For cells with two bud sites we saw an increase in unipolar budding

11

243   from 67% to 84% (Fig. 4D). For cells with three bud sites, it increased from 23% to 43%

244   (Fig. 4E). The increase in unipolar budding was associated with local cell densities of

245   5.2×10^6 and 8.2×10^7 cells/ml, respectively, which signifies the critical cell density under

246   high nitrogen. These values are of the same order of magnitude as the low nitrogen

247   critical cell density (4.8×10^6 and 5.3×10^7 cells/ml). Between 20 and 30 hours in high

248   nitrogen we were not able to observe many cells with three bud sites (Fig. 4E) due to

249   the cell density becoming so high that single buds were no longer visible in the images.

250   For this reason, we did not see a statistically significant increase in the budding pattern

251   between 0 to 10 hours and 20 to 30 hours.

252   Media from the time series experiment in high nitrogen was also analysed by ^{1}H

253   NMR to obtain compound concentrations over time. A list of compounds identified in our

254   high nitrogen samples and their concentrations can be seen in Table 2. Here the

255   metabolite concentrations which corresponded to the observed switch in budding

256   pattern were 1-propanol (1.4 – 3.4 µM), 2-hydroxyisovalerate (0.4 – 0.5 µM), 2-

257   oxoglutarate (1.5 – 2.0 µM), 2-phenylethanol (0.4 – 0.6 µM), acetaldehyde (2.0 – 18.0

258   µM), acetate (27 - 186 µM), acetoin (1.0 – 5.6 µM), fumarate (0.3 – 0.4 µM), isoamylol

259   (0.7 – 0.9 µM), isopropanol (0.3 – 2.9 µM), malate (2.1- 2.2 µM), pyruvate (11.5 – 38.8

260   µM), succinate (0.9 – 1.6 µM), and tyrosol (0.3 – 0.6 µM).

261   Comparing these values to the concentration of metabolites produced under low

262   nitrogen at 20 hours of growth, the alcohols 2-phenylethanol and tyrosol were 60% and

263   63% lower under higher nitrogen respectively, while 1-propanol, isoamylol, and

264   isopropanol concentrations were equivalent. The concentrations of some acids were

265   also lower under high nitrogen, this included the acids 2-hydroxyisovalerate (↓62%), 2-

266   oxogluatare (↓79%), fumarate (↓73%), malate (↓68%) and succinate (↓87%). However,

267   acetate and pyruvate were 16% and 27% higher in the high nitrogen, respectively. Thus,

268   while the same budding pattern behaviour was observed in the different nitrogen

269   conditions, there were significant differences in the metabolome. Collectively, these high

270   nitrogen findings concur with the conditioned media results that physiological

271   metabolites are not responsible for the observed increase in unipolar budding.

272   **Proposed signalling molecule, 2-phenylethanol, can induce unipolar budding at**

273   **high concentrations.**

274   Exogenous 2-phenylethanol has been reported to induce cellular signalling in *S.*

275   *cerevisiae* (14, 19), but at much higher concentrations than those observed in growth

276   media. In order to investigate the effects of these non-physiological concentrations, we

277   added a high concentration of 2-phenylethanol used in previous studies to stimulate

278   filamentous growth (14) to low nitrogen media. Here we observed 91% unipolar budding

279   for two bud sites (Fig. 3A) and 43% for three bud sites (Fig. 3B). These proportions of

280   unipolar budding corresponded to the higher percentage of observed in both time series

281   experiment between 10 to 20 hours; 84-91% for two bud sites (Fig. 2D and 4D) and 37-

282   43% for three bud sites (Fig. 2E and 4E). Furthermore, the proportion of unipolar

283   budding observed for the high 2-phenylethanol condition was significantly higher than

284   the values observed in both the critical cell density and conditioned media conditions;

285   71% for two bud sites (Fig. 3A) and 18-23% for three bud sites (Fig. 3B). These results

286   indicate that a high non-physiological concentration of 2-phenylethanol can recapitulate

287   the increase in unipolar budding, while physiological concentrations do not.

13

DISCUSSION

288

289   The transition to filamentous growth has been proposed as a cell density

290   dependent, chemically mediated switch in *S. cerevisiae*. This conclusion was drawn

291   from studies which examined the growth of yeasts, metabolites, and exogenous

292   compounds, but work has not conclusively shown the dependency of cellular density,

293   induction, and accumulation of a chemical signal (23).

294   The objective of this study was to address the research gaps in the transition to

295   filamentous growth in *S. cerevisiae.* Specifically, we focused on the switch to

296   filamentous growth at a critical quorum sensing molecule concentration corresponding

297   to a critical cell density, and that the intercellular signalling molecule concentrations

298   used to induce the response were physiologically relevant (23). To achieve this, we

299   designed a new methodology to correlate the filamentous growth of *S. cerevisiae* to

300   both cell density and metabolite concentration. We combined chemical cell

301   immobilisation in liquid media, automated time-lapse scanning microscopy, cell counting

302   and ^{1}H NMR. Filamentous yeast cells show a significantly higher proportion of unipolar

303   budding overall compared to non-filamentous cells (1, 7). Thus, by using changes in

304   budding pattern as a proxy for filamentous growth, this study was able to identify the

305   critical cell density at which the cells switched morphology and correlate this to the

306   physiological concentrations of metabolites present.

307   The use of the oCelloScope^{TM} for imaging enabled us to clearly observe the

308   budding pattern of single yeast cells over time. Previous work has applied this imaging

309   technique to bacteriological studies on real-time detection of bacterial growth and

310   antimicrobial susceptibility (32), and to quantify filamentous bacteria (33). The

14

311   methodology of monitoring yeast budding patterns presented in this paper is unique

312   since previous studies have used photomicrographs of developing pseudohyphae in

313   colonies growing on agar (1) or calcofluor staining of bud scars (3, 7). However, growth

314   on agar plates does not allow the monitoring of metabolite production, budding pattern,

315   and cell density simultaneously over time (1, 11, 14), and calcofluor staining does not

316   permit reliable assignment of the birth end of cells (7, 17).

317   The highest proportion of unipolar budding measured here for cells with two bud

318   sites was 85-91% (Fig. 2D and 4D). This finding is in accordance with previous studies

319   that observed >85% unipolar buds for filamentous cells (1, 7). Conversely, in cells with

320   three bud sites we found a maximum of 36-43% unipolar budding (Fig. 2E and 4E).

321   Even though we saw a significant increase over time, this proportion was relatively low

322   compared to the expected 97% from previous findings (7). A possible explanation for

323   this might be that prior studies have not always reported on the position of third bud

324   sites (1) and/or have tended to concentrate on cells at the periphery of the colony (1, 7).

325   Our experiment analysed the whole population of cells which could explain this lower

326   proportion. Additionally, our cells were in the exponential phase of growth and growing

327   in liquid culture, while previous studies used cells in the stationary phase (14) or

328   investigated the budding pattern of colonies growing on agar (1, 7).

329   *S. cerevisiae* strain S288c has a mutation in a gene required for filamentous

330   growth (FLO8)(34) and therefore acted as our negative control for filamentation.

331   Additionally, it is a haploid and thus expected to bud in a consistently axial manner (3,

332   4). Our findings are consistent with this since we observed S288c to bud axially at all

333   time points under both high and low nitrogen conditions. Additionally, as anticipated for

15

334 a diploid able to display filamentous growth, we observed strain Σ1278b to bud only in a

335 bipolar or unipolar way. Furthermore, Σ1278b was observed to increase in unipolar

336 budding, which suggests a transition to filamentous growth (1, 3-6). Our study is the first

337 to identify the cell density at which the cells switch to a filamentous budding pattern. We

338 define this cell density as the critical cell density, and when converted to local cell

339 densities, we find it to be in the range of 4.8×10^6 and 5.3×10^7 cells/ml for low nitrogen.

340 Local cell densities are a more accurate representation of the cell density experienced

341 by the cells in our experiments, as all were immobilised to the bottom of the wells.

342 We sought to obtain the physiological metabolite concentrations when the cells

343 switch to filamentous growth. For our growth phases, these were the metabolite

344 concentrations present between 10 and 20 hours of incubation. We were able to

345 correlate this physiological concentration of metabolites present with the critical cell

346 density and identified a total of 29 compounds in our media (Table 1). This is

347 comparable to other metabolome yeast studies using ^{1}H NMR which identified 18-39

348 total compounds (35-39). The actual number of metabolites produced by *S. cerevisiae* is

349 likely to be in the range of 600-1000 (40, 41). Our observed metabolome may be

350 somewhat limited by the sensitivity of NMR spectroscopy. It should be noted, however,

351 that the highest number of identified compounds achieved using currently available

352 techniques, such as GC-TOF-MS, ranges from 80 (42) to 110 (43), so much more

353 research needs to be done before having any overview of the full yeast metabolome

354 and the physiological concentrations present when cells switch to filamentous growth.

355 Experiments to probe the mechanisms of the observed change in budding

356 pattern were carried out with the Σ1278b strain under low nitrogen conditions. These

16

357   conditions were chosen for comparison with previous studies that have used nitrogen

358   deficiency to induce filamentous growth (1, 11, 14). Here, to investigate the effects of

359   cell density and metabolites independently, an overnight culture growing in YPD broth

360   was directly diluted to an inoculation concentration that corresponded to the critical cell

361   density (Fig. 6A). In contrast to the time series experiment (Fig. 5A), there was no

362   previous cell growth and metabolization for 10 hours in the media. Collectively, results

363   from these experiments suggested that neither the critical cell density alone, nor a

364   combination of critical cell density and physiological metabolites, could recapitulate the

365   increase in unipolar budding pattern (Fig. 3A and B). The difference in the growth

366   environment and metabolism between the different experiments could explain why we

367   saw no change in budding pattern in either of these conditions. The observed change in

368   budding pattern is therefore linked to the specific growth environment found in the time

369   series experiment.

370   Some small molecule alcohols have been associated with induction of

371   filamentous growth through a quorum sensing mechanism whereby their production is

372   autoinduced under low nitrogen. The identified alcohols are tyrosol, 2-phenylethanol and

373   tryptophol (14, 19-21). We were unable to demonstrate a correlation between these

374   alcohols and the change in budding pattern. Both tyrosol and 2-phenylethanol did not

375   show a significant increase in concentration until 30 hours under low nitrogen and had

376   very low concentrations prior to that (Table 1). Since the increase in unipolar budding

377   occurred between 10 and 20 hours (Fig. 2D and E) we concluded that tyrosol and 2-

378   phenylethanol could not induce the change in budding pattern. Furthermore, tryptophol

379   was not identified in our samples, though we specifically looked for it during the NMR

17

380   metabolite identification stage. Tryptophol could have been present but at very low

381   concentrations and non detectable to the ^{1}H NMR. M. Avbelj et al. (21) found that

382   tryptophol was only detectable at a conc of less than 5 μM when cells reached approx.

383   1.5×10^7 cells/ml. Since our cells ended their growth at a lower cell density than this, it is

384   likely that tryptophol was present but at a non-detectable concentration. Finally, all three

385   alcohols have relatively low volatility (2-phenylethanol bp_{760} =219°C (44), tyrosol bp_{760}

386   =139°C (45), and tryptophol bp_{760} = 416°C (46)) thus the measured concentrations were

387   not likely to be inaccurate due to loss during the experiment. The accumulated evidence

388   in this paper indicates that these alcohols are not responsible for triggering the increase

389   in unipolar budding. The discrepancy with previous studies may be attributed to

390   differences in experimental design and execution. For example, our experiment was

391   carried out in liquid media for 30 hours instead of colonies growing on agar plates for 3 -

392   5 days (11, 14, 19).

393   Nutrient deficiencies, including nitrogen (1, 14), amino acids (18) and glucose (8,

394   16) have commonly been linked to inducing filamentous growth in *S. cerevisiae*.

395   Contrary to expectations, in both nitrogen rich and deficient conditions we saw a

396   significant increase in unipolar budding between 10 to 20 hours of growth (Fig. 2B-E,

397   3B-E) occurring at local cell densities of a similar order of magnitude (between 5.2×10^6

398   and 8.2×10^7 cells/ml for high nitrogen and 4.8×10^6 and 5.3×10^7 cells/ml for low nitrogen).

399   Therefore, nutrient deficiency alone appears not to trigger the switch to unipolar budding

400   and perhaps the switch relies on other factors. Furthermore, we see that the metabolite

401   concentrations between the two nitrogen conditions are significantly different (Table 1

18

402   and 2). This provides extra support to our conclusion that the measured metabolites are

403   not triggering the increase in unipolar budding.

404   The results presented in this study have important implications in terms of

405   satisfying the necessary criteria to be classified as a quorum sensing mechanism.

406   Specifically the criteria that filamentous growth is triggered at a critical cell density and is

407   reproducible at physiological signal molecule concentrations (23). Therefore, our

408   findings that the critical cell density and physiological metabolite concentration are not

409   responsible for the shift to a filamentous budding pattern leads to the conclusion that

410   this phenomenon is not occurring through a quorum sensing mechanism but is being

411   controlled in an alternative way. While the change in budding pattern observed in the

412   time series experiment appears to be cell density dependent, it does not however align

413   with an authentic quorum sensing mechanism based on the previously defined criteria.

414   It is only when the cells could increase in cell density in the same media over time that

415   this shift to unipolar budding was observed. These findings raise intriguing questions

416   regarding the mechanism of action controlling this transition to filamentous growth and

417   highlight the need for further studies into this important issue.

418   An alternative mechanism could be one involving cell-to-cell-contact that was

419   found to be a mechanism of growth arrest in yeast (47, 48). Cellular communication

420   mediated by direct cell-to-cell contact has also been found in bacteria. For example,

421   direct cell-to-cell contact results in growth inhibition in *Escherichia coli* (49), coordinates

422   cellular motility in Mycobacterium (50), and mediates auto aggregation and

423   adhesiveness in *Lactobacillus acidophilus* cell surface (51). Thus, there may be a signal

424   present on the cell surface, only present there because of metabolism, that signals the

425   change in budding pattern. Further investigation is therefore required to determine the

426   mechanism by which the cells increase in unipolar budding since there appears to be

427   more transpiring than a quorum sensing mechanism.

428   As mentioned above, 2-phenylethanol has previously been linked to inducing

429   filamentous growth under low nitrogen conditions (14, 19). In these previous

430   experiments, the compound was added at concentrations much higher than those

431   produced by the cells growing in defined media (14, 19, 20). When we used a high non-

432   physiological concentration of 2-phenylethanol, 20 µM compared to the maximum of 4.3

433   µM measured in our low nitrogen media, we observed a shift to unipolar budding. Thus,

434   a high concentration of 2-phenylethanol induced an increase in unipolar budding

435   whereas physiological levels of both 2-phenylethanol and other metabolites did not in

436   our experiments. This finding confirms the association between 2-phenylethanol and

437   filamentous growth. However, an implication of the non-physiological concentration

438   used is that 2-phenylethanol-induced filamentous growth cannot be occurring through a

439   quorum sensing mechanism as previously suggested (14, 21). Table 3 directly

440   compares our 2-phenylethanol findings with the criteria defined by M. Winters et al. (23)

441   and finds it does not satisfy two key points. Therefore, we hypothesise that 2-

442   phenyethanol induces filamentous growth through a toxicity mechanism due to its high

443   concentration rather than through an intercellular signalling mechanism.

444   A recent study by B. A. Lenhart et al. (52) also provides evidence contrary to

445   previous assumptions of quorum sensing mechanisms in *S. cerevisiae.* They found that

446   the induction of morphogenesis by high concentrations of 2-phenylethanol and

447   tryptophol (100 µM) is not observed in most environmental isolates and that the

448   filamentous induction response in Σ1278b was small compared to the extent of that

449   reported by H. Chen and G. R. Fink (14). This supports our conclusion that quorum

450   sensing controlled filamentous growth in yeast is not straightforward and that the

451   mechanism of this biologically critical phenomenon requires more examination.

452   The contribution of this study has been to provide clarity of this transition in the

453   model and industrially useful species, *S. cerevisiae*, highlighting the need for further

454   investigation to determine the mechanism controlling the shift to filamentous growth

455   under physiological conditions. It thus challenges the assumptions around quorum

456   sensing in *S. cerevisiae* widely accepted in literature. The mechanism by which the

457   switch to filamentous growth occurs in *S. cerevisiae* needs to be elucidated through

458   further research without resorting to categorisation into quorum sensing mechanisms.

459   Furthermore, this paper supplies a new methodology of investigating filamentous growth

460   by using budding pattern as a proxy. This may be used to further develop understanding

461   in studies of dimorphism and signalling in other important yeast strains and species.

MATERIALS AND METHODS

462

463   **Yeast Strains & Media.**

464   The *Saccharomyces cerevisiae* strains S288c and Σ1278b were used as a

465   negative and positive control for filamentation respectively (Fig. 5A). The strains were

466   maintained using accepted protocols, detailed below.

467   Yeast Extract Peptone Dextrose (YPD) broth was made by combining 1 g yeast

468   extract (BD Bacto^{TM}, Herlev, Denmark), 2 g bacteriological peptone and 2 g glucose per

469   100 ml of distilled water. The solution was stirred with heating until dissolved. 2 % YPD

21

470   agar plates were made in the same way but with addition of 2g/100ml bacteriological

471   agar to the YPD broth before autoclaving. Synthetic Low Ammonium Dextrose (SLAD)

472   broth was made by combining 0.67 g Yeast Nitrogen Base without amino acids and

473   ammonium sulphate (BD Difco^{TM}, Herlev, Denmark), 2 g glucose and 50 µl of

474   ammonium sulphate solution (1M) per 100 ml of distilled water. Synthetic Ammonium

475   Dextrose (SAD) liquid broth was made by combining 0.67 g Yeast Nitrogen Base

476   without amino acids and ammonium sulphate, 2 g glucose and 3.7 ml of ammonium

477   sulphate solution (1M) per 100 ml of distilled water. All media was autoclaved and

478   cooled to room temperature and sterile filtered (Q-Max 25 mm 0.22 µm CA) before use.

479   Concanavalin A (biotin conjugate, Type IV) at 1mg/ml MilliQ water (Con A) was used for

480   chemical immobilization of cells. All chemicals were purchased from Sigma–Aldrich

481   (Søborg, Denmark).

482   **Image Acquisition.**

483   Images of growing cells in liquid media were obtained using an oCelloScope^{TM}

484   (BioSense Solutions ApS, Farum, Denmark). The oCelloScope^{TM} is a digital time-lapse

485   microscopy technology that generates very clear images of growing microorganisms.

486   This is achieved by scanning through a sample to produce a series of images using a

487   tilted imaging plane. Combining the tilted images give the best focus images and a time-

488   lapse of single cells over time (32, 33).

489   **Time series investigation of budding pattern under low & high nitrogen**

490   **conditions.**

491   S288c and Σ1278b strains of *S. cerevisiae* (Fig. 5A) were used in the time series

492   experiment which linked budding pattern with cell density and physiological metabolite

22

493   concentrations. Figure 5B represents a schematic of the overall time series

494   experimental process used in this research. The experiment was carried out in both high

495   (SAD) and low nitrogen (SLAD) liquid media with the same starting cell density of 10^3

496   cells/ml (Fig. 5C). The overnight culture was made by inoculating 5 ml of YPD broth in a

497   15 ml centrifuge tube with a single yeast colony grown on a 2% YPD agar plate. This

498   was incubated overnight at 25°C with shaking. After overnight incubation, the cells were

499   counted using a hemocytometer (Neubauer Improved counting chamber, Assistent),

500   washed twice with the relevant media, and diluted to obtain a cell density of 1×10^3

501   cells/ml in the relevant media. Three 5 ml stock cultures were made in 15 ml centrifuge

502   tubes with lids to produce biological replicates A, B and C for each condition (Fig. 5C).

503   During the experiment these stock cultures grew at 25°C without shaking. Wells of the

504   12-well microtiter plate (VWR 734-2324 T C-treated 12-well plates) were prepared just

505   before inoculation and imaging by coating the bottom of each well with 15 µl of Con A

506   and allowing the wells to dry. 1 ml of each stock culture was pipetted into wells of the

507   microtiter plate. After inoculation with the cell suspension the plate was placed in the

508   oCelloScope^{TM} and allowed to rest for 30 minutes before starting image acquisition.

509   This was to ensure that the cells were all immobilized on the bottom of the well before

510   imaging to aid focusing. Scanning was set to take place every 10 minutes for 10 hours

511   with one scan area per well at 25°C. Two scan areas per well was used for final 20-to-

512   30-hour time point due to the higher cell density. After 10 hours of image acquisition, the

513   plate was removed, the media collected, spun down in a centrifuge and the supernatant

514   collected and stored at -80° for ^{1}H NMR analysis. Direct transfer of 1 ml of each stock

515   solution occurred again at 10 and 20 hours to a freshly Con A coated microtiter plate, as

516   previously described. Images at 10 and 20 hours were acquired as previously

517   described. Thus, this process resulted in a total of 30 hours of imaging to give three

518   image acquisitions time periods of 10 hours each. Cell density of the stock cultures was

519   also measured at 10, 20 and 30 hours with a hemocytometer.

520   **Investigating the factors responsible for change in budding pattern**

521   Figure 6A represents a schematic of the overall process for the experiments used

522   to investigate the effect of various factors of interest on the budding pattern. This

523   included investigating the effect of critical cell density, conditioned media and high 2-

524   phenylethanol concentrations (Fig. 6B). All experiments were carried out using a cell

525   density which corresponded to the critical cell density identified in the low nitrogen time

526   series experiment ($2x10^4$ cells/ml)

527   **Effect of critical cell density alone on budding pattern.**

528   To test the effect of cell density on the budding pattern, we analyzed the effect of

529   using cells at the critical cell density in low nitrogen broth. The critical cell density

530   condition used SLAD media inoculated with the critical cell density of $2x10^4$ cells/ml

531   (Fig. 6B). 5 ml of YPD broth in a 15 ml centrifuge tube was inoculated with a single

532   yeast colony grown on a 2% YPD agar plate and incubated overnight at 25°C with

533   shaking. After overnight incubation, the cells were counted using a hemocytometer to

534   obtain their cell density. These cells were then washed twice with SLAD media. A cell

535   density of $2x10^4$ cells/ml (critical cell density) was obtained to make three 1 ml solutions

536   (Fig. 6A). This produced three biological replicates, A, B and C. The microtiter plate was

537   prepared as in the time series experiment. The three 1 ml solutions were pipetted into

538   the relevant wells before analysis. Image acquisition in the oCelloScope^{TM} and image

24

539   analysis to obtain the budding pattern was carried out as in the time series budding

540   pattern assay.

Investigating the combined effect of critical cell density and metabolites on
541

budding pattern.
542

543   To test the effect of critical cell density and metabolites on budding pattern. This

544   was done by inoculating the critical cell density of $2x10^4$ cells/ml into conditioned media

545   grown for 20 hours (Fig. 6B). Conditioned media was produced by growing 10^3 cells/ml

546   of freshly washed cells in SLAD broth for 20 hours followed by centrifugation and

547   supernatant removal. This conditioned media supernatant was used immediately in the

548   experiment to wash and inoculate cells, as described in the previous section.

Investigating the effect of non-physiological 2-phenylethanol on budding pattern
549

550   To investigate the effect of non-physiological concentrations of 2-phenylethanol

551   on the budding pattern we used SLAD broth containing 20 µM of 2-phenylethanol. This

552   concentration was previously found to induce filamentation by H. Chen and G. R. Fink

553   (14) under low nitrogen. Cells were inoculated into the spiked broth at the critical cell

554   density of $2x10^4$ cells/ml (Fig 3B). Cell preparation, inoculation and imaging was carried

555   out as described in the previous section.

Image analysis to obtain budding pattern.
556

557   Manual image analysis was carried out on the images acquired from the

558   oCelloScope™ to determine the budding patterns of individual cells. Firstly, the scan

559   areas were cropped using a custom-made code in MATLAB such that thirty images

560   were cropped from each scan area from the three biological replicate wells. Each

561   cropped image was then analyzed by eye to determine the bud site sequence of new

25

562   daughter cells over each period of image acquisition to obtain a bud site sequence for

563   >200 cells and >300 bud sites for each condition (Fig. 1A). This was done by observing

564   new daughter cells and recording the positions of the first two or three bud sites

565   (dependent on the number of times the cell budded within the time frame) to assign

566   each cell with a bud site sequence. An example of this process on a representative cell

567   can be found in Fig 1B (for full time-lapse see Movie S1). These were then assigned

568   their corresponding budding pattern classification (axial, bipolar or unipolar) according to

569   Figure 1A. The budding pattern assignments were then analyzed to determine the

570   percentage value of each budding pattern for the different experimental conditions.

Cell Density Data Analysis

572   Cell densities were averages of three biological replicates. As mentioned above,

573   the cell density in the 1 ml (V_{sample}) of stock solution was determined before imaging by

574   counting with a hemocytometer. This measured cell density value can be converted to a

575   local cell density that the cells would experience based on being immobilized on the

576   bottom of the well. By using the following values, the measured cell density (Measured

577   CD) was recalculated to obtain a local density (Local CD).

578   Assuming a yeast cell size of 10 µm, we calculated the volume that the yeasts

579   would occupy at the bottom of the well. Since the well had a bottom surface area of 3.85

580   cm^2, the new volume occupied by the yeast at the bottom of the well would be 3.85×10^{-3}

581   cm^3 (V_{bottom}) if the whole bottom surface was covered with yeast. This value was used to

582   convert the cell-density per ml value to a local cell density according to the following

583   formula:

$$Local\ CD = \frac{Measured\ CD \times V_{sample}}{V_{bottom}}$$

NMR Chemicals & Buffer Preparation

584

585   Analytical grade sodium phosphate monobasic (NaH2PO3, ≥99.0%), sodium

586   phosphate dibasic dihydrate (Na$_2$HPO$_3$, 2 H$_2$O, ≥98.0%), sodium azide (NaN$_3$, ≥99.5%),

587   deuterium oxide (D$_2$O, 99.9 atom % D), and 3-trimethyl-silyl-[2,2,3,3-2H4] propionic acid

588   sodium salt (TSP-d4, 98 atom % D) were purchased from Sigma–Aldrich (Søborg,

589   Denmark). Water used throughout the study was purified using a Millipore lab water

590   system (Merck KGaA, Darmstadt, Germany) equipped with a 0.22 mm filter membrane.

NMR Sample Preparation

591

592   An aliquot of 700 µL of sample was transferred into a 2 mL Eppendorf tube

593   containing 300 µL of phosphate buffer (0.15 M, 20% D2O). The mixture was vigorously

594   vortexed for 30 s. A volume of 600 µL was transferred into 5 mm O.D. NMR SampleJet

595   tubes (Bruker Biospin, Ettlingen, Germany).

NMR Measurements

596

597   Proton (^{1}H) NMR spectra were recorded on a Bruker Avance III 600 operating at

598   a proton's Larmor frequency of 600.13 MHz. The spectrometer was equipped with a 5

599   mm broadband inverse (BBI) probe and an automated sample changer (SampleJet™,

600   Bruker Biospin, Ettlingen, Germany). The SampleJet was equipped with a refrigerated

601   sample storage station with cooling racks (278 K) and heating/drying station (298 K).

602   Data acquisition and processing were carried out in the TopSpin software (version 3.5,

603   Bruker, Rheinstetten, Germany). Automation of the overall measurement procedure was

604   controlled by iconNMR™ (Bruker Biospin, Rheinstetten, Germany). NMR spectra were

27

605   measured at 298 K using the standard pulse sequence for pre-saturation of the water

606   signal (zgcppr pulse program, Bruker nomenclature), a 90° pulse, a sweep width of

607   9615.385 Hz (16 ppm), and an acquisition time of 3 s. The relaxation delay (d1) was set

608   to 4 s. The receiver gain (RG) value was determined experimentally for each sample.

609   NMR data was collected into 32 K data points after 512 scans. Each free induction

610   decay was apodized by a Lorentzian line-broadening of 0.3 Hz. Automatic phase and

611   baseline correction were performed in TopSpin.

612   **Processing of the NMR data and metabolites quantification**

613   NMR spectra were imported into the SigMa software (31) where the ^{1}H NMR

614   signals were referenced to the TSP signal at 0.00 ppm. Signals alignment and

615   quantification (relative) were performed in SigMa by icoshift and multivariate curve

616   resolution, respectively (53, 54). The yeast metabolome database (http://www.ymdb.ca/)

617   and the Chenomx NMR suite (Chenomx Inc. Edmonton, Canada) were used for

618   metabolite identification.

619   Metabolite concentrations (absolute) were calculated using the following

620   equation:

621
$$C(X) = \frac{Area(X)}{Area(Ref)} * \frac{H(Ref)*C(Ref)}{H(X)}$$

622   Where C(X) is the concentration of the metabolite X, Ref is the reference compound

623   (TSP), and H indicates the number of protons giving rise to the signal from metabolite X

624   and the reference compound (TSP).

625   Due to the short recycle delay (D1) employed for the ^{1}H NMR experiments

626   (D1=4) - too short for an accurate absolute quantification of TSP (D1≥20) - metabolite

28

627   concentrations (absolute) were calculated in two-steps: firstly, the average glucose

628   concentration in the raw media (known) was used to retrieve an estimate of the TSP

629   concentration (absolute) in the very same samples. Secondly, the average absolute

630   concentration of TSP was used to calculate the metabolite concentrations (absolute) in

631   the remaining samples. Therefore, metabolites concentrations reported in the present

632   study are to be considered as estimates of absolute concentrations.

633   **Statistical Analysis**

634   Statistical analyses were performed using Minitab® 19.2020.1 (64-bit). To

635   determine statistically significant differences between conditions of budding pattern

636   proportions, a 2x2 contingency table using Fisher's Exact Test at a significance level of

637    $p=0.05$ was applied. For metabolite concentrations, a minimum of two biological

638   replicates were averaged, and standard deviations calculated to determine the standard

639   error of the mean.

ACKNOWLEDGEMENTS

648   We declare that we have no conflict of interest.

649   Experiment designed by MW, KH and NA; experiment and analysis carried out by

650   MW; NMR data collected by VA; paper written by MW. All authors have read, critically

651   revised, and approved the final version of the manuscript.

652   **REFERENCES**

653   Notes on citations

654   1.   Gimeno CJ, Ljungdahl PO, Styles CA, Fink GR. 1992. Unipolar cell divisions in the yeast S.
655   cerevisiae lead to filamentous growth: Regulation by starvation and RAS. Cell 68:1077-1090.
656   2.   Ceccato-Antonini SR, Sudbery PE. 2004. Filamentous growth in Saccharomyces cerevisiae.
657   Brazilian Journal of Microbiology 35:173-181.
658   3.   Chant J, Pringle JR. 1995. Patterns of bud-site selection in the yeast Saccharomyces cerevisiae.
659   The Journal of cell biology 129:751-765.
660   4.   Freifelder D. 1960. Bud position in Saccharomyces cerevisiae. Journal of bacteriology 80:567.
661   5.   Gimeno CJ, Fink GR. 1992. The logic of cell division in the life cycle of yeast. Science 257:626.
662   6.   Madden K, Costigan C, Snyder M. 1992. Cell polarity and morphogenesis in Saccharomyces
663   cerevisiae. Trends in Cell Biology 2:22-29.
664   7.   Kron SJ, Styles CA, Fink GR. 1994. Symmetric cell division in pseudohyphae of the yeast
665   Saccharomyces cerevisiae. Molecular biology of the cell 5:1003-1022.
666   8.   Cullen PJ, Sprague GF. 2000. Glucose depletion causes haploid invasive growth in yeast.
667   Proceedings of the National Academy of Sciences 97:13619-13624.
668   9.   Dickinson J. 2008. Filament formation in Saccharomyces cerevisiae — a review. Folia
669   Microbiologica 53:3-14.
670   10.   Lengeler KB, Davidson RC, D'souza C, Harashima T, Shen W-C, Wang P, Pan X, Waugh M,
671   Heitman J. 2000. Signal transduction cascades regulating fungal development and virulence.
672   Microbiology and Molecular Biology Reviews 64:746-785.
673   11.   Lorenz MC, Cutler NS, Heitman J. 2000. Characterization of alcohol-induced filamentous growth
674   in Saccharomyces cerevisiae. Molecular Biology of the Cell 11:183-199.
675   12.   Cali BM, Doyle TC, Botstein D, Fink GR. 1998. Multiple functions for actin during filamentous
676   growth of Saccharomyces cerevisiae. Molecular Biology of the Cell 9:1873-1889.
677   13.   Karunanithi S, Joshi J, Chavel C, Birkaya B, Grell L, Cullen PJ. 2012. Regulation of mat responses
678   by a differentiation MAPK pathway in Saccharomyces cerevisiae. PLoS One 7:e32294.
679   14.   Chen H, Fink GR. 2006. Feedback control of morphogenesis in fungi by aromatic alcohols. Genes
680   & Development 20:1150-1161.
681   15.   Gancedo JM. 2001. Control of pseudohyphae formation in Saccharomyces cerevisiae. FEMS
682   microbiology reviews 25:107-123.
683   16.   Lambrechts MG, Bauer FF, Marmur J, Pretorius IS. 1996. Muc1, a mucin-like protein that is
684   regulated by Mss10, is critical for pseudohyphal differentiation in yeast. Proceedings of the
685   National Academy of Sciences 93:8419-8424.
686   17.   Cullen PJ, Sprague Jr GF. 2002. The roles of bud-site-selection proteins during haploid invasive
687   growth in yeast. Molecular biology of the cell 13:2990-3004.

688   18.   Braus GH, Grundmann O, Bruckner S, Mosch H-U. 2003. Amino acid starvation and Gcn4p
689   regulate adhesive growth and FLO11 gene expression in Saccharomyces cerevisiae. Molecular
690   biology of the cell 14:4272-4284.
691   19.   González B, Vázquez J, Cullen PJ, Mas A, Beltran G, Torija M-J. 2018. Aromatic Amino Acid-
692   Derived Compounds Induce Morphological Changes and Modulate the Cell Growth of Wine
693   Yeast Species. Frontiers in Microbiology 9:1-16.
694   20.   González B, Vázquez J, Morcillo-Parra MÁ, Mas A, Torija MJ, Beltran G. 2018. The production of
695   aromatic alcohols in non-Saccharomyces wine yeast is modulated by nutrient availability. Food
696   Microbiology 74:64-74.
697   21.   Avbelj M, Zupan J, Kranjc L, Raspor P. 2015. Quorum-Sensing Kinetics in Saccharomyces
698   cerevisiae: A Symphony of ARO Genes and Aromatic Alcohols. Journal of Agricultural and Food
699   Chemistry 63:8544-8550.
700   22.   Monds RD, O'Toole GA. 2008. Metabolites as intercellular signals for regulation of community-
701   level traits, p 105-129. In Winans S, Bassler B (ed), Chemical Communication Among Bacteria.
702   American Society of Microbiology, Washington, DC.
703   23.   Winters M, Arneborg N, Appels R, Howell K. 2019. Can community-based signalling behaviour in
704   Saccharomyces cerevisiae be called quorum sensing? A critical review of the literature. FEMS
705   Yeast Research 19.
706   24.   Miller M, Bassler B. 2001. Quorum Sensing in Bacteria. Annual Review of Microbiology 55:165-
707   199.
708   25.   Henke JM, Bassler BL. 2004. Bacterial social engagements. Trends in Cell Biology 14:648-656.
709   26.   Fuqua C, Winans SC, Greenberg EP. 1996. Census and Consensus in Bacterial Ecosystems: The
710   LuxR-LuxI Family of Quorum-Sensing Transcriptional Regulators. Annual Review of Microbiology
711   50:727-751.
712   27.   Kleerebezem M, Quadri LEN, Kuipers OP, De Vos WM. 1997. Quorum sensing by peptide
713   pheromones and two-component signal-transduction systems in Gram-positive bacteria.
714   Molecular Microbiology 24:895-904.
715   28.   West SA, Winzer K, Gardner A, Diggle SP. 2012. Quorum sensing and the confusion about
716   diffusion. Trends in Microbiology 20:586-594.
717   29.   Wuster A, Babu MM. 2008. Chemical Molecules that Regulate Transcription and Facilitate Cell-
718   to-Cell Communication, p 1-8. In Begley TP (ed), Wiley Encyclopedia of Chemical Biology
719   doi:doi:10.1002/9780470048672.wecb501. John Wiley & Sons, New Jersey.
720   30.   Dickinson J. 1996. Fusel alcohols induce hyphal-like extensions and pseudohyphal formation in
721   yeasts. Microbiology 142:1391-1397.
722   31.   Khakimov B, Mobaraki N, Trimigno A, Aru V, Engelsen SB. 2020. Signature Mapping (SigMa): An
723   efficient approach for processing complex human urine 1H NMR metabolomics data. Analytica
724   Chimica Acta.
725   32.   Fredborg M, Andersen KR, Jørgensen E, Droce A, Olesen T, Jensen BB, Rosenvinge FS,
726   Sondergaard TE. 2013. Real-Time Optical Antimicrobial Susceptibility Testing. Journal of Clinical
727   Microbiology 51:2047.
728   33.   Fredborg M, Rosenvinge FS, Spillum E, Kroghsbo S, Wang M, Sondergaard TE. 2015. Automated
729   image analysis for quantification of filamentous bacteria. BMC Microbiology 15:255.
730   34.   Liu H, Styles CA, Fink GR. 1996. Saccharomyces cerevisiae S288C Has a Mutation in FL08, a Gene
731   Required for Filamentous Growth. Genetics 144:967-978.
732   35.   Puig-Castellví F, Alfonso I, Piña B, Tauler R. 2015. A quantitative 1 H NMR approach for
733   evaluating the metabolic response of Saccharomyces cerevisiae to mild heat stress.
734   Metabolomics 11:1612-1625.

36. Nilsson M, Duarte IF, Almeida C, Delgadillo I, Goodfellow BJ, Gil AM, Morris GA. 2004. High-resolution NMR and diffusion-ordered spectroscopy of port wine. Journal of agricultural and food chemistry 52:3736-3743.

37. Peng C, Viana T, Petersen MA, Larsen FH, Arneborg N. 2018. Metabolic footprint analysis of metabolites that discriminate single and mixed yeast cultures at two key time-points during mixed culture alcoholic fermentations. Metabolomics 14:93.

38. Kumar Babele P. 2019. Zinc oxide nanoparticles impose metabolic toxicity by de-regulating proteome and metabolome in Saccharomyces cerevisiae. Toxicology Reports 6:64-73.

39. Lourenço AB, Roque FC, Teixeira MC, Ascenso JR, Sá-Correia I. 2013. Quantitative 1H-NMR-Metabolomics Reveals Extensive Metabolic Reprogramming and the Effect of the Aquaglyceroporin FPS1 in Ethanol-Stressed Yeast Cells. PLOS ONE 8:e55439.

40. Raamsdonk LM, Teusink B, Broadhurst D, Zhang N, Hayes A, Walsh MC, Berden JA, Brindle KM, Kell DB, Rowland JJ. 2001. A functional genomics strategy that uses metabolome data to reveal the phenotype of silent mutations. Nature biotechnology 19:45-50.

41. Mo ML, Palsson BØ, Herrgård MJ. 2009. Connecting extracellular metabolomic measurements to intracellular flux states in yeast. BMC Systems Biology 3:37.

42. Ding M-Z, Zhou X, Yuan Y-J. 2010. Metabolome profiling reveals adaptive evolution of Saccharomyces cerevisiae during repeated vacuum fermentations. Metabolomics 6:42-55.

43. Kim S, Lee DY, Wohlgemuth G, Park HS, Fiehn O, Kim KH. 2013. Evaluation and optimization of metabolome sample preparation methods for Saccharomyces cerevisiae. Analytical chemistry 85:2169-2176.

44. Alfa Aesar. 2021. A15241 2-Phenylethanol, 98+%. https://www.alfa.com/en/catalog/A15241/. Accessed 6 August.

45. Alfa Aesar. 2021. A14891 2-(4-Hydroxyphenyl)ethanol, 98%. https://www.alfa.com/en/catalog/A14891/. Accessed 10 August.

46. Alfa Aesar. 2021. L02555 Tryptophol, 97%. https://www.alfa.com/en/catalog/L02555/. Accessed 8 August.

47. Nissen P, Arneborg N. 2003. Characterization of early deaths of non-Saccharomyces yeasts in mixed cultures with Saccharomyces cerevisiae. Archives of Microbiology 180:257-263.

48. Nissen P, Nielsen D, Arneborg N. 2003. Viable Saccharomyces cerevisiae cells at high concentrations cause early growth arrest of non-Saccharomyces yeasts in mixed cultures by a cell–cell contact-mediated mechanism. Yeast 20:331-341.

49. Aoki SK, Pamma R, Hernday AD, Bickham JE, Braaten BA, Low DA. 2005. Contact-dependent inhibition of growth in Escherichia coli. Science 309:1245-1248.

50. Kaiser D. 2004. Signaling in myxobacteria. Annu Rev Microbiol 58:75-98.

51. Kos B, Šušković J, Vuković S, Šimpraga M, Frece J, Matošić S. 2003. Adhesion and aggregation ability of probiotic strain Lactobacillus acidophilus M92. Journal of applied microbiology 94:981-987.

52. Lenhart BA, Meeks B, Murphy HA. 2019. Variation in filamentous growth and response to quorum-sensing compounds in environmental isolates of Saccharomyces cerevisiae. G3: Genes, Genomes, Genetics 9:1533-1544.

53. Savorani F, Tomasi G, Engelsen SB. 2010. icoshift: A versatile tool for the rapid alignment of 1D NMR spectra. Journal of magnetic resonance 202:190-202.

54. De Juan A, Jaumot J, Tauler R. 2014. Multivariate Curve Resolution (MCR). Solving the mixture analysis problem. Analytical Methods 6:4964-4976.

781 **TABLES & FIGURES**
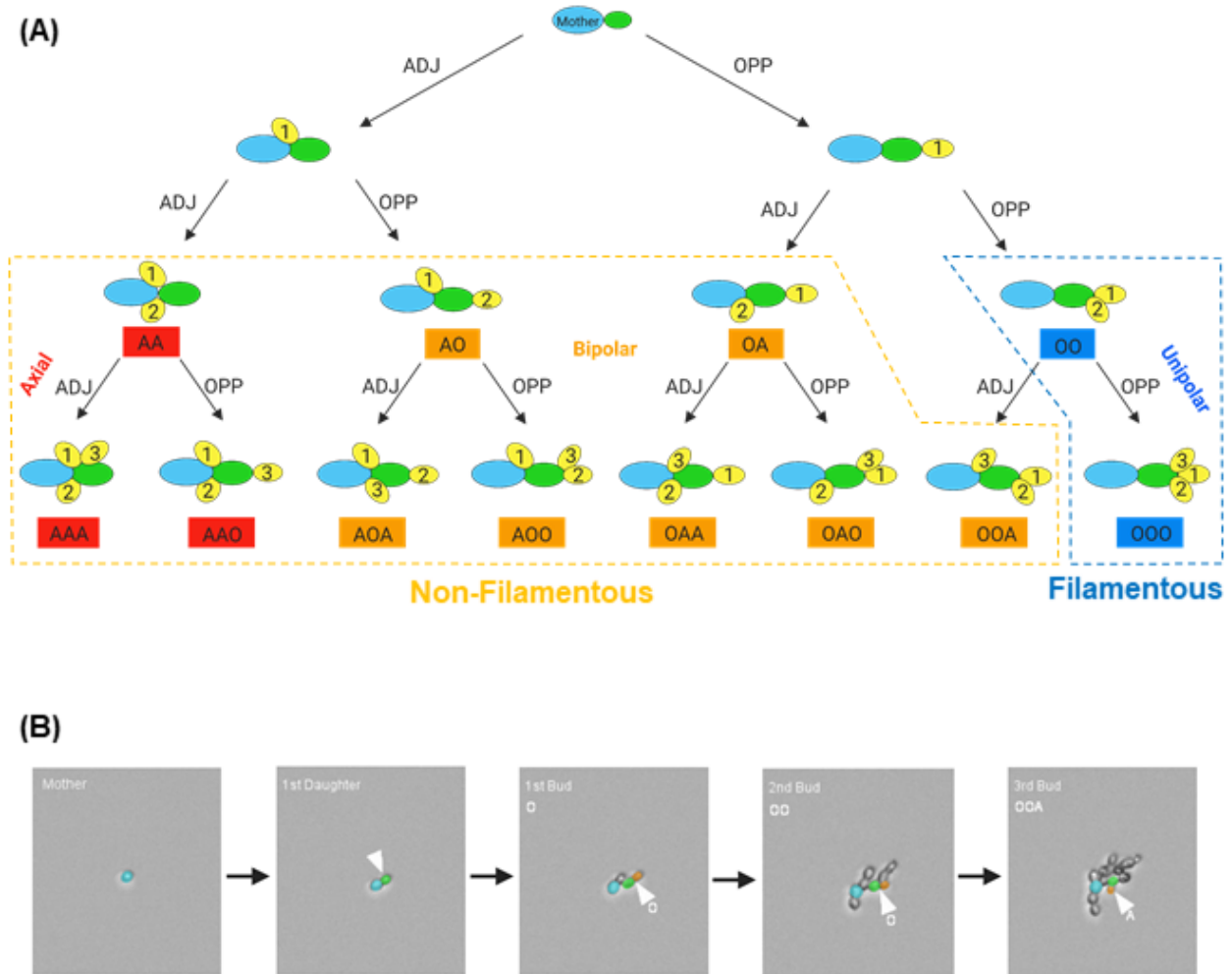
782
783 **FIG 1** Bud site sequence categorisation to budding pattern. (A) All potential BSS
784 labelled with their corresponding budding pattern (axial = red, bipolar = orange, unipolar
785 = blue). Bud site sequence is assigned and categorised to a corresponding budding
786 pattern for daughters with both two and three bud sites as shown. For cells growing in
787 yeast-form, haploids will adopt an axial pattern, defined as new buds emerging
788 consistently adjacent to the junction to the mother. Diploids will adopt a bipolar pattern
789 whereby buds may emerge either adjacent or opposite the junction to the mother. When
790 filamentous growth occurs, both cell types transition to a unipolar budding pattern
791 defined as bud sites emerging consistently from the end opposite the junction to the
792 mother. In this way, budding pattern can be used as a proxy for tracking filamentous
793 growth in liquid media. (B) Example of a cropped image cell being classified by its
794 budding pattern. For the 1st daughter (green), the first bud (orange) emerges opposite
795 the birth end, followed by a second bud also opposite its birth end and finally the third
796 bud emerges adjacent to the birth end. Thus, this daughter would have a bud site
797 sequence of OOA which classifies it as bipolar budding pattern according to Fig 1A.

33
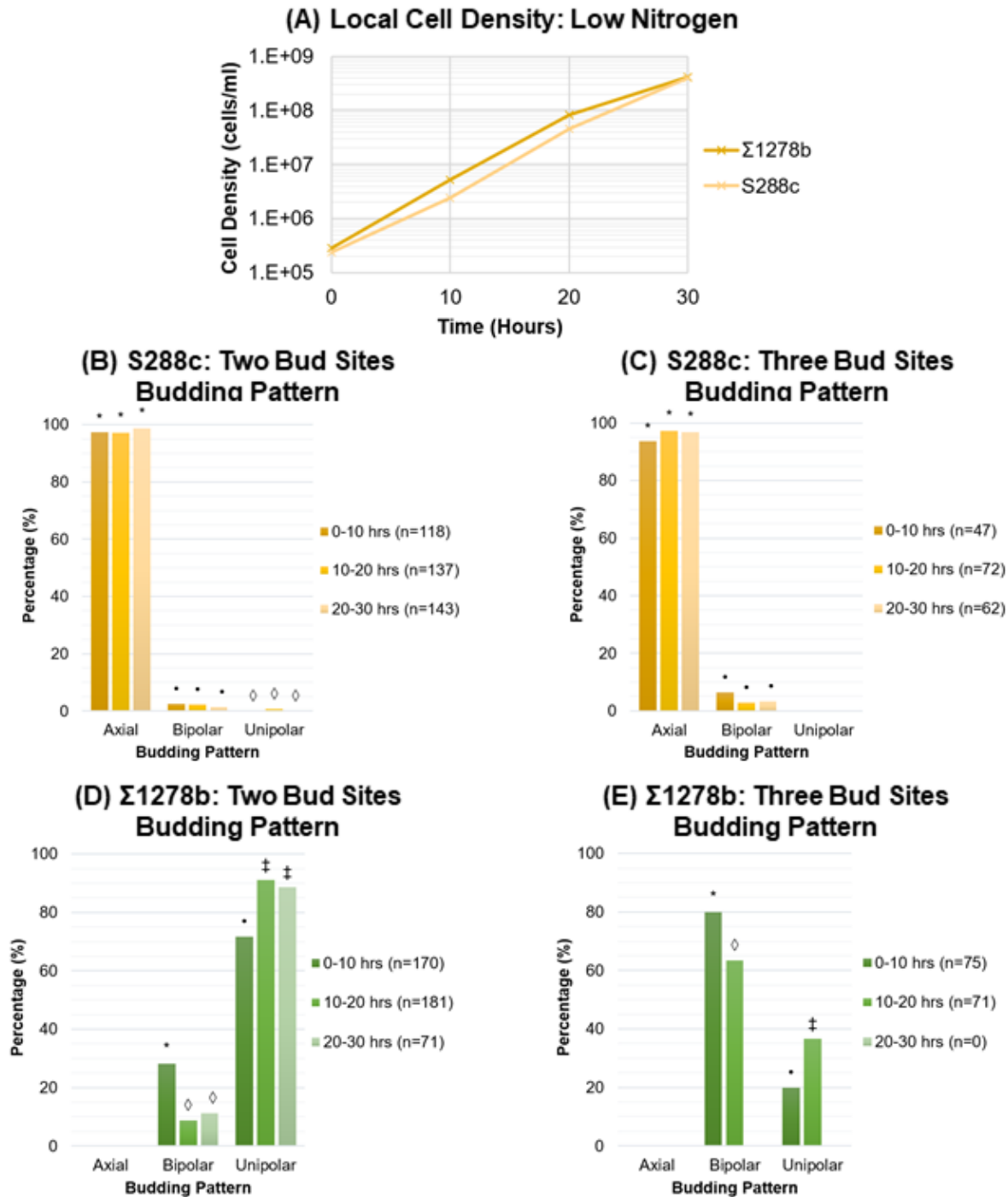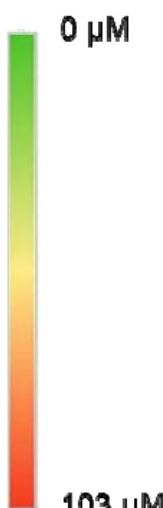
FIG 2 The budding patterns of yeast in <u>low nitrogen </u>liquid media can be tracked during growth and correlated to cell density. (A) Changes in local cell density of S288c and Σ1278b showed a similar pattern. (C-E) Budding pattern results displayed as a percentage of total cells counted for two bud sites in *S. cerevisiae* strains S288c (B) and Σ1278b (C) and for three bud sites in strains S288c (D) and Σ1278b (E). Statistically significant differences at p=0.05 between time points are marked with different symbols.

TABLE 1: Heatmap of the physiological concentrations of compounds detected in low nitrogen (SLAD) media during growth of Σ1278b strain of *S. cerevisiae* over time[a]

Low Concentration Metabolites (µM)			
Metabolite Name	**0 hrs**	**10 hrs**	**20 hrs**	**30 hrs**
1-Propanol	0.8 ± 0.1	1.4 ± 0.3	3.7 ± 0.3	6.7 ± 0.5
2-Hydroxyisovalerate	0.6 ± 0.2	0.7 ± 0.2	1.3 ± 0.8	2.9 ± 0.2
2-Oxoglutarate	3.4 ± 1.2	4.4 ± 0.2	9.3 ± 2.5	61.7 ± 1.3
2-Phenylethanol	0.5 ± 0.1	0.7 ± 0.2	1.5 ± 0.8	4.3 ± 0.4
3-Methylxanthine	5.9 ± 0.8	3.9 ± 0.1	4.2 ± 0.4	3.7 ± 0.2
Acetaldehyde	0.4 ± 0.1	2.3 ± 0.3	19.2 ± 0.6	30.0 ± 3.8
Acetoin	0.4 ± 0.1	6.7 ± 4.7	8.0 ± 2.1	20.1 ± 1.3
Choline	2.3 ± 0.2	2.9 ± 0.9	2.0 ± 0.8	1.6 ± 0.4
Diacetyl	5.0 ± 0.4	5.4 ± 0.4	4.8 ± 0.8	5.0 ± 0.1
Fumarate	0.6 ± 0.1	0.5 ± 0.2	1.1 ± 0.5	14.6 ± 1.4
Glycolate	110.7 ± 3.3	112.8 ± 10.3	101.8 ± 24.3	118.1 ± 2.0
Hydroxyacetone	3.6 ± 1.6	4.2 ± 1.7	2.4 ± 0.2	3.3 ± 0.1
Isoamylol	0.6 ± 0.2	0.6 ± 0.4	1.0 ± 0.7	11.1 ± 1.1
Isopropanol	0.3 ± 0.1	0.4 ± 0.1	2.1 ± 0.2	4.8 ± 0.7
Malate	2.4 ± 0.6	2.9 ± 0.4	6.8 ± 3.7	10.2 ± 0.7
Methionine	0.2 ± 0.1	0.2 ± 0.1	0.6 ± 0.1	1.0 ± 0.1
Myoinositol	47.3 ± 1.0	43.6 ± 7.3	33.1 ± 13.0	41.4 ± 0.7
Niacin	9.5 ± 0.2	7.8 ± 1.6	7.6 ± 2.9	9.6 ± 0.2
Pantothenate	4.3 ± 0.2	4.8 ± 0.4	5.3 ± 0.6	6.0 ± 0.1
Pyridoxine	7.8 ± 0.2	8.3 ± 0.3	7.8 ± 0.3	7.4 ± 0.1
Pyruvate	4.9 ± 0.9	5.0 ± 0.1	30.6 ± 1.5	52.8 ± 1.9
Succinate	1.8 ± 0.2	2.5 ± 0.1	12.0 ± 7.3	45.0 ± 0.2
Trehalose	91.3 ± 0.5	88.1 ± 8.3	66.9 ± 26.6	85.9 ± 1.3
Tyrosol	0.2 ± 0.1	0.3 ± 0.1	0.8 ± 0.2	4.9 ± 0.2
Xanthine	0.9 ± 0.1	1.3 ± 0.3	0.6 ± 0.1	6.6 ± 0.1

0 µM

103 µM

High Concentration Metabolites (µM)			
Metabolite Name	**0 hrs**	**10 hrs**	**20 hrs**	**30 hrs**
Acetate	14 ± 4	17 ± 1	160 ± 6	411 ± 12
Ethanol	189 ± 40	369 ± 8	5403 ± 160	14334 ± 1023
Formate	221 ± 2	238 ± 2	231 ± 9	193 ± 4
Glucose (x10³)	107 ± 1	103 ± 1	115 ± 5	99 ± 1

0 µM

[a]Metabolites identified through ^{1}H-NMR and quantified using the SigMa programme (Khakimov et al. 2020). Values are expressed as mean ± SE for two or three biological replicates.
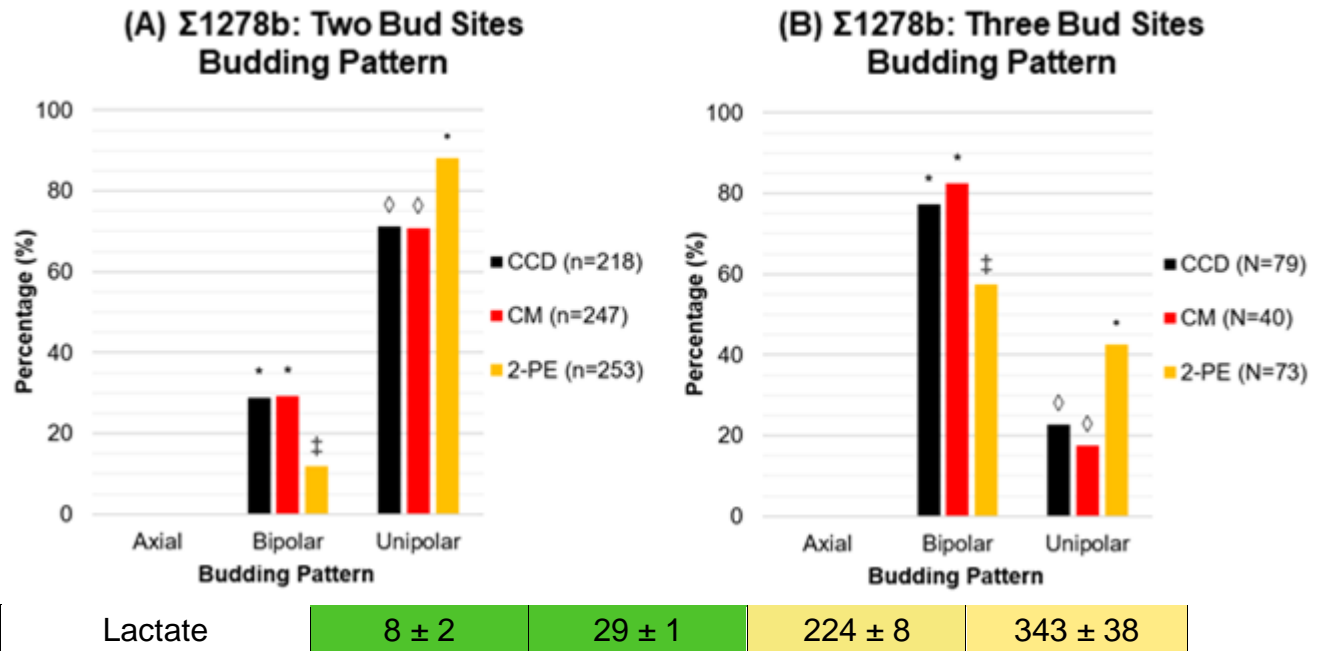
Lactate	8 ± 2	29 ± 1	224 ± 8	343 ± 38

FIG 3 The critical cell density and conditioned media do not induce a shift to unipolar budding under low nitrogen. Experiments carried out using Σ1278b strain under low nitrogen at the critical cell density to attempt to investigate the effect on cell density alone (CCD), cell density and signalling metabolites in combination (CM), and non-physiological 2-phenylethanol (2PE) on the budding pattern. Budding pattern results for two bud sites (A) and three bud sites (B) show that only 2PE can recapitulate the increase in unipolar budding. Statistically significant differences at p=0.05 between time points are marked with different symbols.
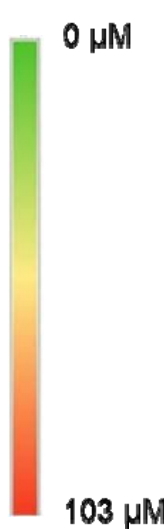
835
836
837
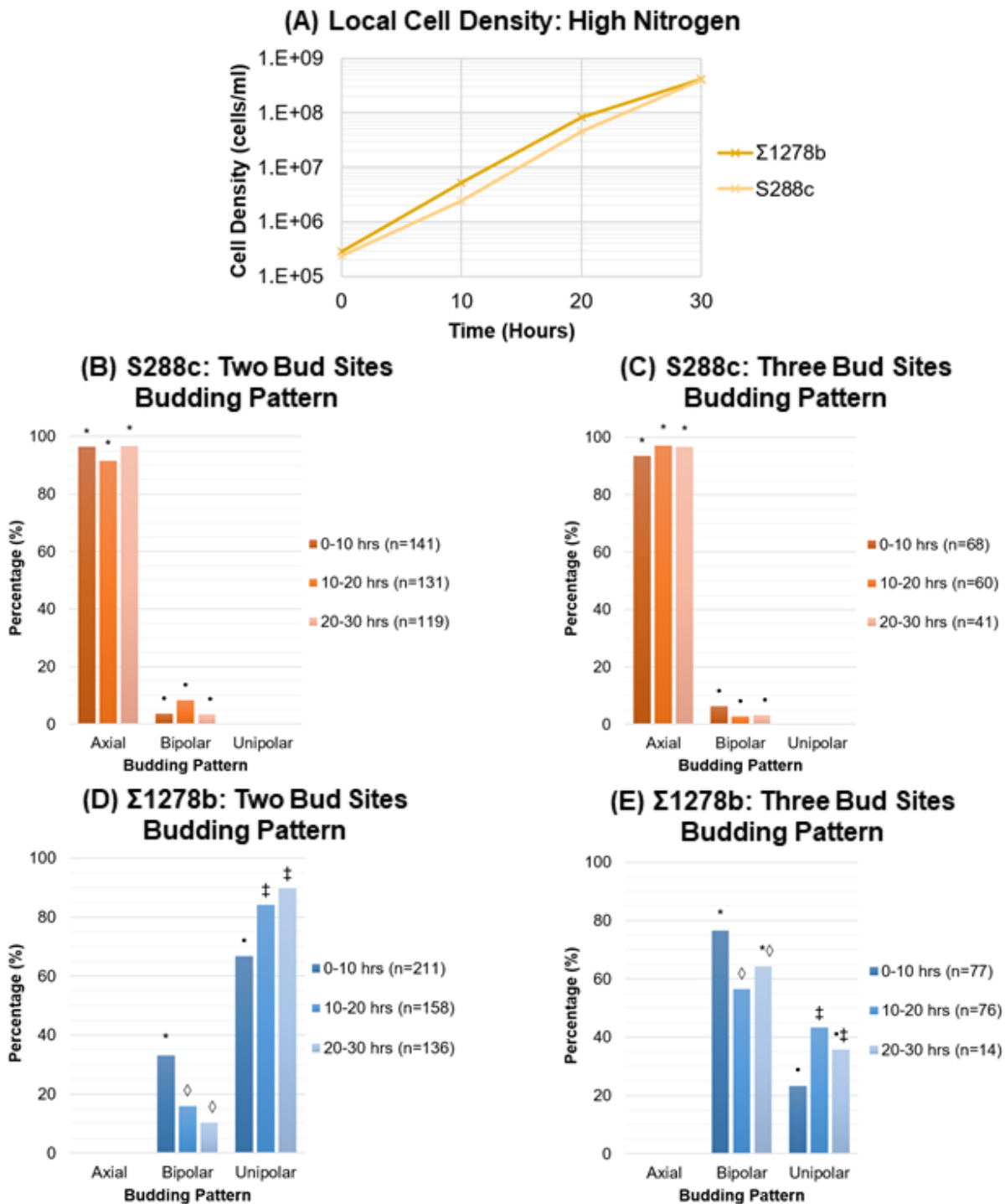
838
FIG 4 The budding patterns of yeast in <u>high nitrogen</u> liquid media show the same behaviour compared to low nitrogen. (A) Changes in local cell density of S288c and Σ1278b showed a similar pattern. (B-E) Budding pattern results displayed as a
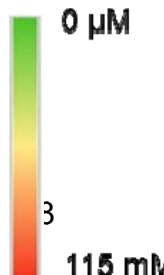
37

842   percentage of total cells counted for two bud sites in *S. cerevisiae* strains S288c (B) and
843   Σ1278b (B) and for three bud sites in strains S288c (D) and Σ1278b (E). Statistically
844   significant differences at p=0.05 between time points are marked with different symbols.
845   ***TABLE 2:*** Heatmap of the physiological concentrations of compounds detected in high
846   nitrogen (SAD) media during growth of Σ1278b strain of *S. cerevisiae* over time[a]

Low Concentration Metabolites (µM)				
Metabolite Name	**0 hrs**	**10 hrs**	**20 hrs**	**30 hrs**
1-Propanol	1.3 ± 0.1	1.4 ± 0.1	3.4 ± 0.4	21.4 ± 10.5
2-Hydroxyisovalerate	0.3 ± 0.1	0.4 ± 0.1	0.5 ± 0.2	1.8 ± 0.3
2-Oxoglutarate	0.7 ± 0.2	1.5 ± 0.1	2.0 ± 0.1	13.6 ± 3.2
2-Phenylethanol	0.4 ± 0.1	0.4 ± 0.1	0.6 ± 0.1	0.9 ± 0.4
3-Methylxanthine	6.9 ± 0.3	7.8 ± 0.1	8.3 ± 0.4	6.7 ± 1.1
Acetaldehyde	1.5 ± 0.4	2.0 ± 0.6	18.0 ± 5.3	18.8 ± 8.8
Acetoin	1.2 ± 0.1	1.0 ± 0.1	5.6 ± 1.9	25.3 ± 15.4
Choline	2.2 ± 0.6	3.9 ± 1.0	3.7 ± 1.0	2.1 ± 0.8
Diacetyl	4.5 ± 0.1	4.5 ± 0.1	4.5 ± 0.2	4.2 ± 0.1
Fumarate	0.2 ± 0.1	0.4 ± 0.1	0.3 ± 0.1	4.8 ± 0.6
Glycolate	102.5 ± 2.1	102.8 ± 3.3	101.9 ± 2.0	85.3 ± 11.0
Hydroxyacetone	8.1 ± 0.1	7.9 ± 0.2	8.1 ± 0.3	8.4 ± 0.2
Isoamylol	0.8 ± 0.1	0.7 ± 0.1	0.9 ± 0.1	13.0 ± 6.6
Isopropanol	0.3 ± 0.1	0.3 ± 0.1	2.9 ± 0.8	2.5 ± 0.8
Malate	3.0 ± 0.3	2.1 ± 0.5	2.2 ± 0.2	6.2 ± 1.1
Methionine	0.2 ± 0.1	0.3 ± 0.1	0.5 ± 0.1	6.8 ± 3.8
Myoinositol	51.3 ± 0.9	50.3 ± 0.7	48.2 ± 1.6	43.7 ± 4.2
Niacin	9.4 ± 0.3	9.4 ± 0.3	11.6 ± 0.9	6.5 ± 1.7
Pantothenate	4.9 ± 0.1	5.3 ± 0.3	5.3 ± 0.2	5.5 ± 0.2
Pyridoxine	8.9 ± 0.2	9.0 ± 0.3	9.6 ± 0.2	10.5 ± 1.1
Pyruvate	8.5 ± 0.8	11.5 ± 0.5	38.8 ± 6.3	92.2 ± 48.2
Succinate	1.4 ± 0.2	0.9 ± 0.1	1.6 ± 0.1	18.5 ± 10.9
Trehalose	95.3 ± 1.5	94.4 ± 2.3	92.0 ± 1.1	64.1 ± 18.6
Tyrosol	0.4 ± 0.1	0.6 ± 0.1	0.3 ± 0.1	0.4 ± 0.1
Xanthine	1.1 ± 0.2	1.3 ± 0.1	1.2 ± 0.4	0.9 ± 0.2

0 µM — 103 µM

847

High Concentration Metabolites (µM)				
Metabolite Name	**0 hrs**	**10 hrs**	**20 hrs**	**30 hrs**
Acetate	32 ± 5	27 ± 2	186 ± 4	639 ± 62
Ethanol	633 ± 265	472 ± 45	4972 ±	43113 ± 22177

0 µM — 115 mM

[a]Metabolites identified through ^{1}H-NMR and quantified using the SigMa programme (Khakimov et

Formate	238 ± 3	220 ± 4	206 ± 6	150 ± 44
Glucose (x10^3)	114± 2	112 ± 2	110 ± 2	102 ± 5
Lactate	24 ± 8	33 ± 5	231 ± 57	848 ± 293

848 **TABLE 3** Analysis of whether our budding pattern shift results observed for *S.*
849 *cerevisiae* strain Σ1278b match the criteria for an intercellular signaling molecule and a
850 quorum sensing molecule[a].
851

	Criteria	**2-phenylethanol**
Intercellular Signalling Molecule	Extracellular & Identified	Y
	Specific signalling mechanism	Y
	Reproducible response	N[b]
	Adaptive at community level	Y
Quorum Sensing Molecule	Proportional to cell density	Y
	Critical threshold trigger	N[c]

852
853 [a] Criteria from (23).
854 [b] Response only observed when 2-phenylethanol used at much higher concentrations
855 (20 µM) than found to be physiologically produced (0.7 – 1.5 µM)
856 [c] Since the response is only induced at high levels it may be a starvation or stress
857 response and not a QS mechanism
858
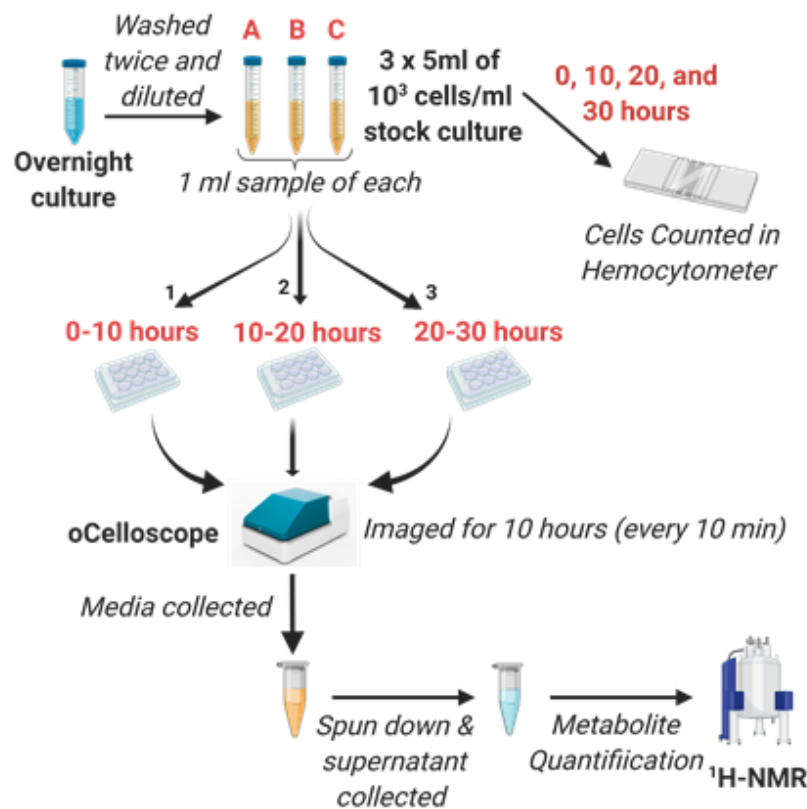859
860
861
862
863
864
865
866
867
868
869
870
871
872
873
874
875

876
877
878
879

(A) Strains of *S. cerevisiae* used in the experiment

Strain Name	Source	Budding Pattern	Filamentation	Reference
S288c	Lab strain	Axial	-	ATCC° 26108™
Σ1278b	NCYC 1391	Bipolar	+	(Grenson, Hou & Crabeel 1970)

(B) Experimental Set-Up

Overnight culture — Washed twice and diluted — A B C — 1 ml sample of each — 3 x 5ml of 10³ cells/ml stock culture — 0, 10, 20, and 30 hours — Cells Counted in Hemocytometer

1 — 0-10 hours
2 — 10-20 hours
3 — 20-30 hours

oCelloscope — Imaged for 10 hours (every 10 min)

Media collected — Spun down & supernatant collected — Metabolite Quantifiication ¹H-NMR

(C) Conditions

Media	Strain	Starting Cell Density (cells/ml)
Low Nitrogen (SLAD)	S288c	
	Σ1278b	
High Nitrogen (SAD)	S288c	1x10³
	Σ1278b	

880 **FIG 5** The budding patterns of yeast in low and high nitrogen liquid media can be
881 tracked during growth and correlated to cell density. (A) Two different strains of S.
882 cerevisiae were used to include a positive and negative control for FG. (B) Schematic of

40

883   the time series that utilised the oCelloScope™ for image acquisition to simultaneously
884   monitor budding pattern, cell density, and metabolite concentration using experimental
885   conditions in (C) to investigate filamentous growth behaviour under low and high
886   nitrogen.
887
888

(A) Experimental Set-Up
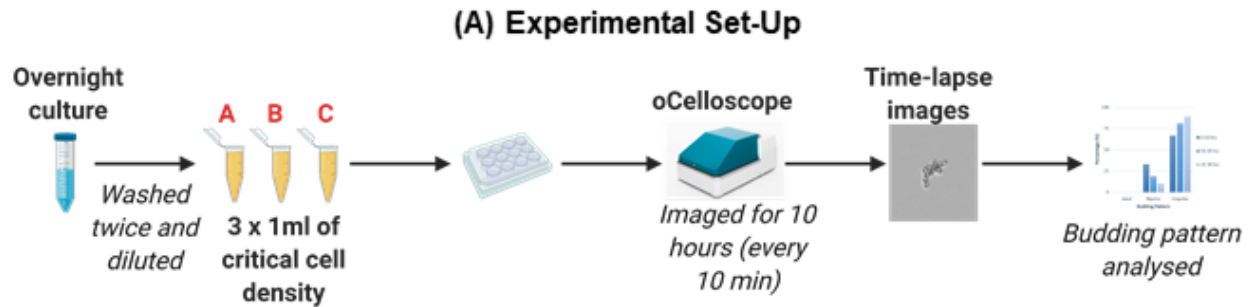
(B) Experiment conditions for investigating the effects of critical cell density, conditioned media and non-physiological 2-phenylethanol on budding pattern.

Label	Description	Strains	Media	Starting Cell Density (cells/ml)
CCD	Critical Cell Density		SLAD	
CM	20 hours CM	Σ1278b	20 hours SLAD conditioned media	2 x 10^4
2-PE	Non-physiological 2-phenylethanol		SLAD + 20 µM 2-phenylethanol	

889
890   **FIG 6** Investigating the factors responsible for change in budding pattern. (A) Schematic
891   diagram of experimental set-up. (B) Experimental conditions used for experiments
892   included the critical cell density (CCD), 20 hours conditioned media (CM), and media
893   with a high concentration of 2-phenylethanol (2PE). All conditions inoculated cells at the
894   critical cell density 2 x 10^4 cells/ml.
895

896

897

898

899

SUPPLEMENTAL MATERIAL

901 **MOVIE S1** Example of cropped image and bud site sequence assignment (BSS). For
902 the 1st daughter, the first bud emerges opposite the birth end, followed by a second bud
903 also opposite its birth end and finally the third bud emerges adjacent to the birth end.
904 Thus, this daughter would have a BSS of OOA which classifies it as bipolar budding
905 pattern according to Figure 1.
906
907 **TABLE S1** Results from Nitrogen Concentration Assay which measured the nitrogen
908 concentration from the media and the supernatant from the three biological replicates A,
909 B and C end of the BPA experiment.
910

| Nitrogen Condition	High Nitrogen				Low Nitrogen			
Condition	Media	A	B	C	Media	A	B	C
Nitrogen Conc (mM)	82.86	79.16	78.87	81.85	1.06	0.06	0.03	0.03

911
912
913 **TABLE S2** ^{1}H-NMR metabolite shifts and intervals with J-coupling. Shifts in bold were
914 used for quantification.
915

Label	Metabolite Name	Shift (ppm)	Multiplicity	J-coupling (hz)	Notes
1	1-propanol	0.88 **1.53** 3.55	t m t	7.5 7.1 (6.6)	
2	2-hydroxyisovalerate	0.83 **0.95** 2.01 3.84	d d m d	6.86 6.94 (13.81,6.88) (3.75)	
3	2-oxoglutaric acid	2.44 **3.01**	t t	6.83 6.82	
4	2-phenylethanol	**2.85** 3.83 7.30 7.37	t t m t	6.7 - - 7.5	
5	3-methylxanthine	3.51 **8.02**	s s		
6	Acetaldehyde	2.25 **9.68**	d q	3.0 3.0	

7	Acetate	**1.92**	s		
8	Acetoin	1.38 **2.22** 4.41	d s q	7.1 7.1	
9	Arabinose	3.51 3.68 3.83 3.90 3.95 4.05 4.50 5.25	dd m dd m m m d d	(9.7,7.8) (9.7, 3.5) 7.7 (3.57)	NQ
10	Choline	**3.18** 3.50 4.05	s dd ddd	 (5.8,4.1)	
11	Diacetyl	**2.31**	s		
12	Ethanol	**1.18** 3.66	t q	7.0 7.0	
13	Formate	**8.45**	s		
14	Fructose	3.58 3.69 3.82 3.90 4.00 4.03 4.12	m m m dd m dd m	 (9.9,3.4) 12.8, 1.0	NQ
15	Fumarate	**6.51**	s		
16	α-glucose	3.81 3.82 3.38 3.70 3.53 5.24	m m m m m d	 3.8	Media nutrient
17	β-glucose	3.89 3.72 3.38 3.45 3.23 **4.63**	m m m m dd d	 (7.8, 9.2) 8.0	Media nutrient
18	Glycolate	**3.96**	s		
19	Hydroxyacetone	**2.16** 3.27 4.26	s s d		

20	Isoamylol	0.86 **1.44** 1.66 3.5 4.3	d q m t s	6.9 7.0	
21	Isopropanol	**1.16** 4.01	d m	6.0	
22	Lactic acid	**1.31** 4.10	d q	7.0 7.0	
23	Malic acid	2.34 **2.66** 4.29	dd dd dd	(15.37,10.2) 15.4, 2.9 (10.23,2.9)	
24	Myo-inositiol	3.26 3.52 3.61 **4.06**	t dd t t	(9.3) 9.7 2.8	Media nutrient
25	Niacin	7.53 8.26 8.61 **8.94**	t d d s	(7.94, 4.90) (4.98, 1.67)	Media nutrient
26	Pantothenate	0.88 **0.92** 2.40 3.37 3.4 3.48 3.51 3.98	s s t s m s s s		Media nutrient
27	Pyridoxine	2.47 4.73 7.69	s s s		
28	Pyruvate	2.38	s		
29	Succinate	2.41	s		
30	Taurine	3.25 3.42	t t	6.1 (6.1)	NQ
31	Trehalose	3.42 3.64 3.75 3.82 5.11	t dd m m d	(9.47) (9.93,3.8) 3.8	
32	Tyrosol	2.77 3.77 6.86 7.17	t t d d	6.7 - 8.4 8.5	

916

917
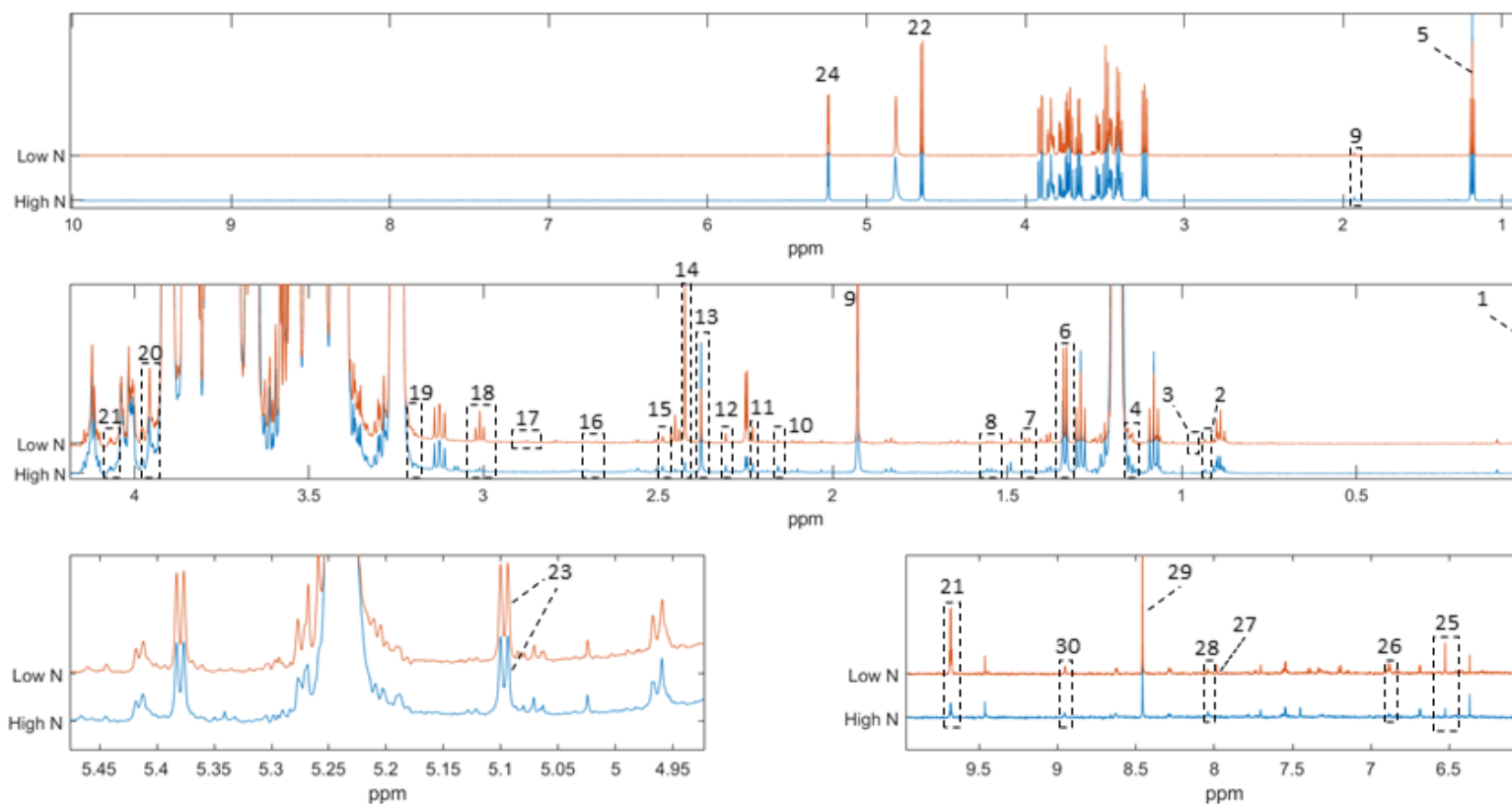
FIG S1 Representative ^{1}H-NMR spectra of samples. The major resonances used for quantification have been assigned: 1. TSP; 2. Pantothenate; 3. 2-hydroxyisovalerate; 4. Isopropanol; 5. Ethanol; 6. Lactate; 7. Isoamylol; 8. 1-Propanol; 9. Acetate; 10. Hydroxyacetone; 11. Acetoin; 12. Diacetyl; 13. Pyruvate; 14. Succinate; 15. Pyridoxine; 16. Malate; 17. 2-Phenylethanol; 18. 2-oxoglutarate; 19. Choline; 20. Glycolate; 21. Myoinositol; 22. β-Glucose; 23. Trehalose; 24. α-Glucose; 25. Fumarate; 26. Tyrosol; 27. Xanthine; 28. 3-Methylxanthine; 29. Formate; 30. Niacin; 31. Acetaldehyde.
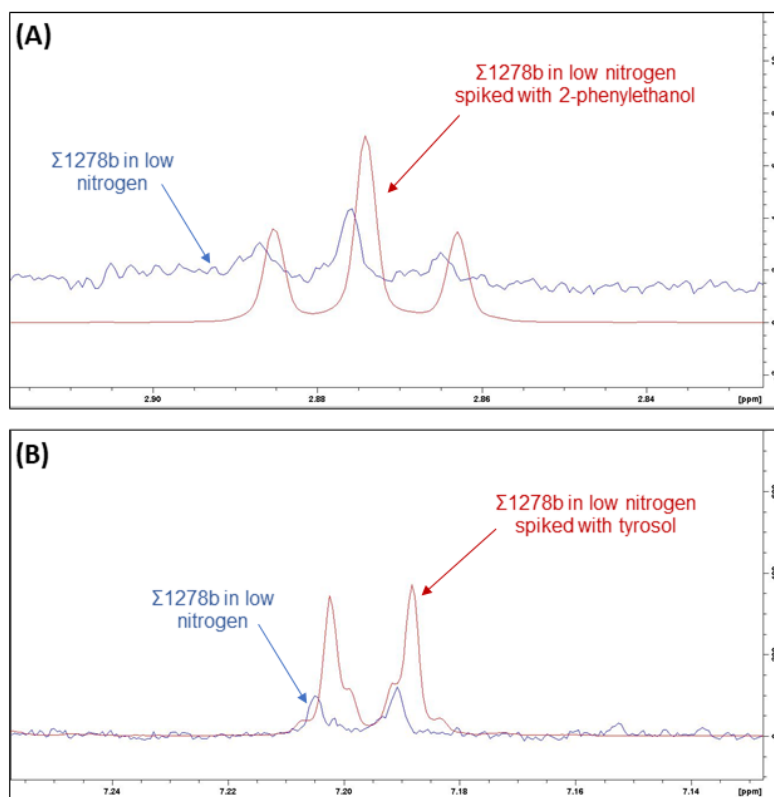
925
926
927
928 **FIG S2** Representative ^{1}H-NMR spectra showing the results of the spiking experiment
929 conducted by adding (A) 10 μL 2-phenylethanol and (B) 5 μL tyrosol to the samples.